

# LWA-HAND: Lightweight Attention Hand for Interacting Hand Reconstruction

Xinhan Di<sup>1</sup> and Pengqian Yu<sup>2</sup>

<sup>1</sup> BLOO Company, Shanghai, China  
xinhan.di@blooxr.com

<sup>2</sup> Independent Researcher, Singapore  
yupengqian1989@gmail.com

**Abstract.** Hand reconstruction has achieved great success in real-time applications such as visual reality and augmented reality while interacting with two-hand reconstruction through efficient transformers is left unexplored. In this paper, we propose a method called lightweight attention hand (LWA-HAND) to reconstruct hands in low flops from a single RGB image. To solve the occlusion and interaction challenges in efficient attention architectures, we introduce three mobile attention modules. The first module is a lightweight feature attention module that extracts both local occlusion representation and global image patch representation in a coarse-to-fine manner. The second module is a cross image and graph bridge module which fuses image context and hand vertex. The third module is a lightweight cross-attention mechanism that uses element-wise operation for cross attention of two hands in linear complexity. The resulting model achieves comparable performance on the InterHand2.6M benchmark in comparison with the state-of-the-art models. Simultaneously, it reduces the flops to  $0.47GFlops$  while the state-of-the-art models have heavy computations between  $10GFlops$  and  $20GFlops$ .

**Keywords:** Interacting hand reconstruction, Efficient transformers, InterHand2.6M

## 1 Introduction

Monocular single hand pose and shape recovery has recently witnessed great success owing to deep neural networks [2,9,19,49,52] in industrial applications such as virtual reality (VR), human-computer-interaction (HCI), robotics, holoportation, and digital medicine. However, two-hand reconstruction is more challenging and remains unsolved for real-world applications such as hand tracking in Figure 1. First, it is difficult for networks to align hand poses with image features as severe mutual occlusions and appearance similarity confuse the feature extractors. In addition, interaction between two-hands is hard to be represented during network training. Finally, it is not trivial to design efficient network architectures which can formulate the occlusion and interaction of two hands and meet the requirement of low latency on mobile hardware at the same time.



**Fig. 1.** Hand tracking application in visual reality. Here interacting hand reconstruction remains a challenge.

Promising results have been produced by the monocular depth-based two-hands tracking methods [20,29,30,38,40]. Although these depth-based frameworks are studied for years, the algorithm complexity limit the ubiquitous application of the methods. Recently, a monocular RGB based two-hand reconstruction by tracking dense matching map is proposed [41]. However, its tracking procedure is inherently sensitive to fast motion and the prior knowledge between interacting hands is not fully used. Since the proposal of the large scale two-hand dataset InterHand2.6M [27], learning based single image two-hands reconstruction methods are well studied. Such examples include the 2.5D heatmaps for hand joint positions estimation [8,17,27] and the attention map for the extraction of sparse and dense image features [45,21]. However, these methods consume a lot of computation power and restrict their applications on mobile devices such as VR/AR glass and robots. In contrast, mobile vision transformers [39,25,26,5] has achieved great success in vision tasks and deployment on mobile devices. The lightweight attention based methods are likely to represent the occlusions and interaction of two-hands on mobile devices.

Motivated by the above mentioned challenges, we propose lightweight attention hand (LWA-HAND), a mobile attention and graph based single image reconstruction method. Firstly, two-stream GCN is utilized to regress mesh vertices of each hand in a coarse-to-fine-manner, similar to traditional GCN [9] and Intaghand [21]. However, for the two-hand reconstruction in a low energy consumption, naively using a two-stream network with normal attention modules

fails to represent occlusion and interaction of two hands in low latency. Moreover, application of normal feature extraction [11] and extra attention modules [21] for contact image and graph features leads to high flops. To address these issues, we equip a lightweight vision transformer for feature extraction of interacting hands. This mobile transformer utilizes the data stream of MobileNet [34] and transformers with a two-way bridge. This bridge enables bidirectional fusion of local features of each hand and global features of contexts of the occlusions and interaction between hands. Furthermore, a pyramid cross domain module is applied to fuse image representation and hand representation in a coarse-to-fine and lightweight manner. Global priors of image domain with very few tokens is calculated in a pyramid way and a direct fusion of the prior and representation of hand is then conducted. Unlike heavy-weight cross hand attention module [21], a separate attention mechanism with linearly complexity [26] reduces the calculation of cross attention to encodes interaction context into hand vertex features. Therefore, the proposed lightweight modules makes the whole network architecture a good choice for resource-constrained devices. Overall, our contributions are summarized as:

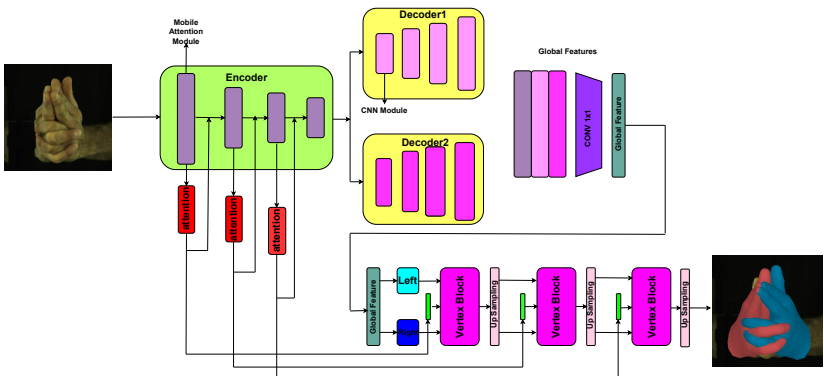


**Fig. 2.** Proposed mobile network architecture. The green block is the mobile attention encoder. The two yellow block are decoders of 2.5D heatmap and 2D segmentation. The stacked bridges represent the attention part (in red), the fusion part (in green) and the vertex attention part (in pink), respectively.

1. We propose a mobile two-hand reconstruction method based on lightweight attention mechanism named LWA-HAND (illustrated in Figure 2) and demonstrate the effectiveness of mobile attention for the two-hand reconstruction task.
2. We propose a lightweight feature attention module to extract both local occlusion representation and global image patch representation in a coarse-to-fine manner, producing fusion of these two representation with low latency.

3. We propose a cross image and graph bridge module to fuse image context and hand vertex. It constructs a pyramid bridge to extract global context features of two hands with very few tokens in the attention mechanism, connecting context features directly to the hand vertex domain without extra transforms of calculation.
4. We propose a lightweight cross attention mechanism which uses element-wise operation for cross attention of two hands with linear complexity [26], reducing the flops of attention operation in the representation of interacting hands.

For the construction of interacting hands, our method reduces the calculation to  $470M$  flops and achieves comparable results with existing solutions based on heavy-weight networks of 10 times of flops on the InterHand 2.6M benchmark. This demonstrates the ability of the mobile transformers in the construction of interacting hands on resource-constrained devices.

## 2 Related Work

### 2.1 Hand Reconstruction

Hand reconstruction is studied for decades, including single hand reconstruction, two-hand reconstruction, and mesh regression. Some of the existing methods are already applied to virtual reality, robots and remote medical operations. The most related work of hand reconstruction is reviewed below.

**Single Hand Reconstruction** Hand pose estimation and gesture recognition are well studied [12,42] before deep learning era. Then, estimation of 3D hand skeleton from a single image has achieved great success [3,28,36,53]. Since the popular parametric hand model MANO [31] and a variety of large scale datasets [15,27,35,54] are available, there are various methods to reconstruct both a hand pose and shape [1,4,9,19,22,37,48,52]. Among all of these methods, the most recent transformer-based models [22,23,21] produce the best results, demonstrating the ability of the attention mechanism to learn the non-local relationship between any two vertices. However, this excellent performance relies on heavy weight attention mechanism which is impractical on mobile devices. Therefore, we propose our methods based on mobile transformers.

**Two-Hand Reconstruction** Although almost all single-hand reconstruction methods could extend to two-hand reconstruction tasks, interacting hands remains a challenge for human motion capture. First, some body and hand simultaneous reconstruction methods [6,16,32,43,50,51] treat each hand in a separate manner and thus are not able to handle close hand interaction cases with heavy occlusion. A recent multi-view tracking based method provides a solution to reconstruct high-quality interactive hand motions, however, its hardware setup is expensive, and the algorithm is time-consuming. Other monocular kinematic

tracking based methods are sensitive to fast motion and possible tracking failure regardless of whether a depth sensor [20,29,30,38,40] or an RGB camera [41] is incorporated. However, their dense mapping strategy queries correspondences between hand vertices and image pixels. In contrast, deep learning based methods [8,17,27,33,47] directly reconstruct per-frame two-hand interaction. They rely on 2.5D heatmaps to estimate hand joint positions [8,27], extract sparse image features [44], reconstruct each hand respectively and fine-tune later [17,32]. However, hands are naturally 3D surfaces, and sparse local image features encoded in the 2.5D heatmaps may not effectively capture hand surface occlusions and hands interaction context. Therefore, dense feature representation based on attention and graph [21] are studied to well learn the occlusion and context in the training. Unfortunately, the normal attention mechanism is computationally expensive and is hard to be deployed on mobile devices. In this paper, we propose several designs of lightweight attention modules to reduce the calculation and energy consumption.

## 2.2 Real-time Hand Reconstruction

Currently, a variety of hand reconstruction methods are applied to mobile devices which require low latency and low energy consumption. In order to drive virtual and augmented reality (VR/AR) experiences on a mobile processor, a variety of hand reconstruction methods are proposed based on mobile network. For example, inverted residuals and linear bottlenecks [34] are used to build base blocks for hand pose, scale and depth prediction [10]. Precise landmark localization of 21 2.5D coordinates inside the detected hand regions via regression is estimated to address CPU inference on the mobile devices [46]. However, these mobile methods based on mobile CNN blocks lack the ability of reconstruct hands with occlusions and interaction. The attention mechanisms and graph is not applied to build representation of local and global context of interacting hands. Therefore, we propose mobile attention and graph modules which can both handle challenging occlusions and interacting context with low flops.

## 3 Formulation

### 3.1 Two-Hand Mesh Representation

Unlike previous two-hand reconstruction methods [17,27,33,48] that use joints or articulated models as hand representations, only surface vertices with a fixed mesh topology of two hands is required. A same mesh topology of the popular MANO [31] model is adopted for each hand which contains  $N = 778$  vertices. To assist the mobile attention mechanism, dense matching encoding for each vertex similar to [41,21] as positional embedding is used. As shown in Figure 2, our LWA-HAND has a hierarchical architecture that reconstructs hand mesh using a variety of coarse-to-fine blocks with different types such as mobile attention module, domain bridges between image context and hand vertex and pyramid hand

vertex decoding modules [21]. To construct the coarse-to-fine mesh topology and enable the building of bridge between image context and hand representation in a coarse-to-fine manner, we leverage the graph coarsening method similar in [21] and build  $N$   $b = 3$  level submeshes with vertex number  $N_0 = 63$ ,  $N_1 = 126$ ,  $N_2 = 252$  and reserve the topological relationship between adjacent levels for upsampling. After the third block, a simple linear layer is employed to upsample the final submesh ( $N_2 = 252$ ) to the full MANO mesh ( $N = 778$ ), producing the final two-hand vertices.

### 3.2 Overview

The proposed system contains three main parts: mobile vision attention encoder-decoder (green block and yellow blocks in Figure 2), pyramid attention-graph bridges (red, green and pink blocks in Figure 2), and mobile interacting attention module (vertex representation in Figure 2). Given a single RGB image, a global feature vector  $F_G$  is firstly produced through feeding it to an mobile vision attention encoder. Simultaneously, several bundled feature maps  $\{Y_t \in \mathbb{R}^{C_t \times H_t \times W_t}, t = 0, 1, 2\}$ , where  $t$  indicates that the  $t$ -th feature level corresponds to the input of the  $t$ -th bridge in the domain bridges,  $H_t \times W_t$  is the resolution of the feature maps which gradually increases, and  $C_t$  is the feature channel. The domain bridges take  $Y_t, t = 0, 1, 2$  as input and transform them to hidden features  $Z_t, t = 0, 1, 2$  through attention operation. Then, the bridges directly fuse global context features  $Z_t, t = 0, 1, 2$  with hand vertex features in a coarse-to-fine manner. Note that, at each lever, the stream runs through a vision mobile attention module, a domain bridge, and a graph decoded module. These modules are illustrated in Figure 2 - Figure 5 and will be discussed in Section 4.1, Section 4.2 and Section 4.3, separately.

## 4 Light Former Graph

Existing work of interacting hands reconstruction [21,45,27] is built with convolutional encoder and attention module with lots of energy consumption. In this paper, we propose a lightweight former graph architecture as shown in Figure 2 to represent the interaction and occlusion of two-hands. The Light former graph is consisted of three main modules based on lightweight blocks including lightweight feature attention module, pyramid cross image and graph bridge module and lightweight cross hand attention module. They are introduced in the following.

### 4.1 Lightweight Feature Attention Module

Lightweight convolutional neural networks (CNNs) such as MobileNets [13,14,34] efficiently encode local features by stacking depthwise and pointwise convolutions. Mobile vision transformers and its follow-ups [7,24,39] achieve global features through tokens. Inspired by the above advantages, a recent mobile archi-

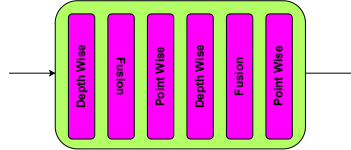


**Fig. 3.** Mobile module with attention.

tureture [5] is applied to connect local features and global features as shown in Figure 3.

This module takes an image as the first input  $\{\mathbf{X} \in \mathbb{R}^{(H \times W \times 3)}\}$  and applies inverted bottleneck blocks [34] to extract local features. Besides, learnable parameters (tokens)  $\mathbf{Z} \in \mathbb{R}^{M \times d}$  are taken as the second input where  $M$  and  $d$  are the number and dimension of tokens, respectively. Similar to [21], these tokens are randomly initialized, and a small number of tokens ( $M < 7$ ) is applied to represent a global prior of the image. Therefore, the operation of inverted bottleneck blocks and tokens results in much less computational effort.

In order to make fusion of the global and local features in the encoder, the lightweight encoding is computed by:

$$F_{X_i^0} = H(F_{X_{i-1}^1}, Z_i) = \text{Fusion}[\text{CNN}_{\text{Depth-wise}}(F_{X_{i-1}^1}), Z_i], \quad (1)$$

$$F_{X_i^1} = H(F_{X_i^0}) = \text{CNN}_{\text{Point-wise}}(F_{X_i^0}), \quad (2)$$

where  $i = 0, 1, 2, 3, \dots, N_{\text{stack}}$ ,  $N_{\text{stack}}$  is the number of stacks,  $X_i^0, X_i^1, i > 0$  are local features of the two stages in the  $i$ -th stack, and  $X_0 = X_0^0 = X_0^1$  represents the input image. Here  $Z_i$  represents the global features in the  $i$ -th stack,  $\text{CNN}_{\text{Depth-wise}}$  represents the depth wise convolution,  $\text{CNN}_{\text{Point-wise}}$  represents the point wise convolution, Fusion represents the contact operation.  $F_{X_i^0}$  represents the feature of the stage 0 at the  $i$ -th stack,  $F_{X_i^1}$  represents the local feature of the stage 1 at the  $i$ -th stack,  $H(F_{X_{i-1}^1}, Z_i)$  represents the convolutional functions with the input  $F_{X_{i-1}^1}$  and  $Z_i$ . The fusion operation directly contact global tokens  $Z_i$  with local features  $\text{CNN}_{\text{Depth-wise}}(X_{i-1}^1)$  rather than other attention mechanism with heavy calculation.

## 4.2 Pyramid Cross Image and Graph Bridge Module

Communication between CNN and transformer through a bridge is an efficient way to produce fusion of different domain representation [25,5]. Moreover, communication between image and graph is demonstrated as an efficient way to feed context features into the representation of hand vertex. The pyramid cross image and graph bridge module build two types of communication: communication between local features and global tokens and communication between global features and hand vertex. Furthermore, the communication between the triple domains is built in a coarse-to-fine manner (see, Figure 4): Firstly, unlike

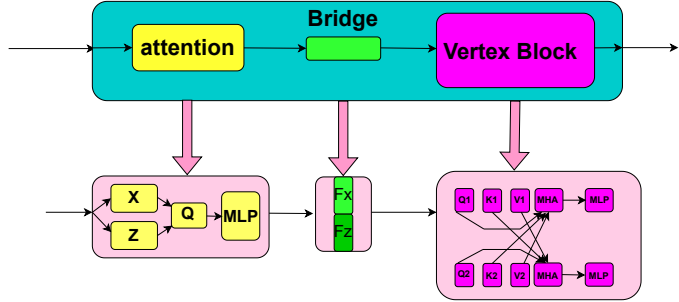


**Fig. 4.** Graph bridge module. The yellow block is the attention module for building an attention map between the local feature  $X$  and the global feature  $Z$  through an attention matrix  $Q$  and MLP module. The fusion module (in green) is the direct contact module for the feature  $F_x$  and  $F_z$ . The pink vertex module is built with cross hand attention module with two  $Q$  matrix  $Q_1$  and  $Q_2$ , two key matrix  $K_1$  and  $K_2$ , two value matrix  $V_1$  and  $V_2$ .

the two-way bridge to connect local and global features [5], the local features and global features are communicated through an one-way bridge. A lightweight cross attention is applied where  $(\mathbf{W}^Q, \mathbf{W}^K, \mathbf{W}^V)$  are the matrices of three projections, only  $\mathbf{W}^Q$  is used. Specifically, the lightweight cross attention from local features map  $\mathbf{X}$  to global tokens  $\mathbf{Z}$  is computed by:

$$A_{F_{X_i^1} \rightarrow Z_i} = [\text{Attn}(\bar{z}_i \mathbf{W}_i^Q, \bar{x}_i, \bar{x}_i)]_{i=1:h} \mathbf{W}^O, \quad (3)$$

where the local feature  $F_{X_i^1}$  and global tokens  $Z_i$  are split into  $h$  heads as  $F_{X_i^1} = [\bar{x}_1, \dots, \bar{x}_h]$ ,  $Z_i = [\bar{z}_1, \dots, \bar{z}_h]$  for multi-head attention. The split for the  $i$ -th head is represented as  $\bar{z}_i \in \mathbb{R}^{M \times \frac{d}{h}}$ ,  $W_i^Q$  is the query projection matrix for the  $i$ -th head, and  $W_o$  is used to combine multiple heads together.

Secondly, at the  $i$ -th stack, the global features  $Z_i$  are mapped to the domain of graph representation in the bridge, denoted as  $M_i$ . Here,  $M_i$  is computed by:

$$M_i = A_{F_{X_i^1} \rightarrow Z_i} F_{X_i^1} \quad (4)$$

where  $A_{F_{X_i^1} \rightarrow Z_i}$  is the attention matrix calculated previously. Here  $F_{X_i^1}$  is the local feature at the  $i$ -th stack and  $Z_i$  is the global feature at the  $i$ -th stack.

The mapping is calculated in two stages: direct connection stage and cross attention stage. At the first stage, the global feature  $M_i$  is directly contacted with hand vertex representation  $V_i$  at the  $i$ -th stage for each hand. At the second stage, a cross attention mechanism is applied between two hands [21] for deep fusion. The two-stage fusion is calculated as the following:

$$V_i^{Ro} = \text{Fusion}(V_i^R, M_i), \quad V_i^{Lo} = \text{Fusion}(V_i^L, M_i), \quad (5)$$

$$FH_i^{R \rightarrow L} = \text{softmax} \left( \frac{f(Q_i^{Lo}) f(K_i^{Ro})}{d} \right) f(V_i^{Ro}), \quad (6)$$

$$FH_i^{L \rightarrow R} = \text{softmax} \left( \frac{f(Q_i^{Ro})f(K_i^{Lo})}{d} \right) f(V_i^{Lo}), \quad (7)$$

where at the  $i$ -th stack,  $V_i^R$  and  $V_i^L$  are the representations of right hand vertex and left hand vertex before fusion,  $V_i^{Ro}$  and  $V_i^{Lo}$  are the representations of right hand vertex and left hand vertex after fusion, the operation of direct contact is applied to make the fusion. Multi-head self-attention (MHSA) module is applied to obtain the query, key and value features of each hand representation  $V_i^{ho}, h \in L, R$  after the fusion, and the values are indicated by  $Q_i^{ho}, K_i^{ho}, V_i^{ho}, h \in L, R$ .  $T$  represents the matrix transpose. Like interacting hands in the existing methods [21],  $FH_i^{R \rightarrow L}$  and  $FH_i^{L \rightarrow R}$  are the cross hand attention features encoding the correlation between two hands.  $d$  is a normalization constant and  $f$  represents the function with the three features as input respectively. The cross-hand attention features are merged into the hand vertex features by a pointwise MLP layer  $fp$  as

$$FH_i^{La} = fp(FH_i^{Lo} + FH_i^{R \rightarrow L}), \quad (8)$$

$$FH_i^{Ra} = fp(FH_i^{Ro} + FH_i^{L \rightarrow R}), \quad (9)$$

where  $FH_i^{La}$  and  $FH_i^{Ra}$  are the output hand vertex features at the  $i$ -th stack, which act as the input of both hands at the next stack.

### 4.3 Lightweight Cross Hand Attention Module

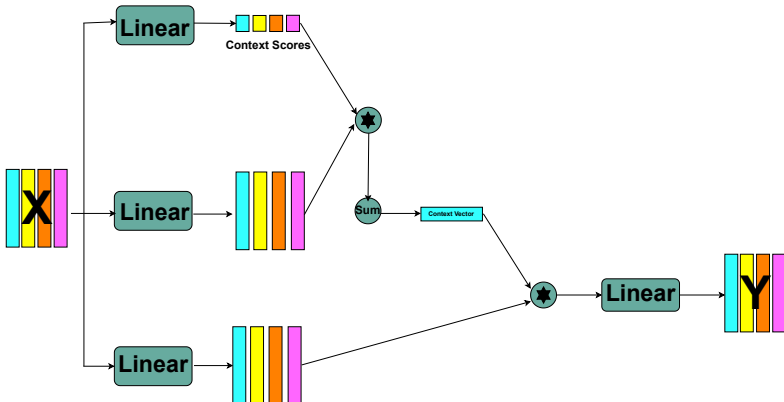


**Fig. 5.** Cross hand attention module.

In order to reduce the calculation of the above mentioned cross attention between two hands, a separable self-attention structure [26] is applied to construct a lightweight cross hand attention module. The input  $FH_i^h, h \in L, R$  is

processed using three branches: input  $I$ , key  $K$  and value  $V$  as shown in Figure 5.

Firstly, the input branch  $I$  is responsible to calculate the value of query features  $Q_i^{ho}, h \in L, R$ . The input branch  $I$  maps each  $d$  dimensional token in  $FH_i^{ho}, h \in L, R$  to a scalar using a linear layer with weights  $W_i^I \in \mathbb{R}^d$ . This linear projection is an inner-product operation and computes the distance between latent token  $L$  and  $FH_i^h$ , resulting in a  $k$ -dimensional vector. A softmax operation is then applied to this  $k$  dimensional vector to produce context scores  $c_s \in \mathbb{R}^k$  representing the value of query features.

Secondly, the context scores  $c_s$  are used to compute a context vector  $c_v$ . Specifically, the input  $FH_i^h$  is linearly projected to a  $d$  dimensional space using  $K$  branch with weights  $W_k \in \mathbb{R}^{d \times d}$  to produce an output  $FH_{ik}^h \in \mathbb{R}^{k \times d}$  representing the value of key features. The context vector  $c_v \in \mathbb{R}^d$  is then computed as a weighted sum of  $FH_{ik}^h$ :

$$c_v = \sum_{i=1}^k c_s(i) FH_{ik}^h(i). \quad (10)$$

Finally the contextual information encoded in  $c_v$  is shared with all tokens in  $FH_i^h$ . The input  $FH_i^h$  is linearly projected to a  $d$  dimensional space using the value branch  $V$  with wights  $W_v \in \mathbb{R}^{d \times d}$  to produce an output  $FH_{iv}^h$  representing the value of the value features.

#### 4.4 Loss Function

For training the proposed mobile network, we utilize vertex loss, regressed joint loss and mesh smooth loss. It is similar to IntagHand [21].

**Vertex Loss** We use  $L1$  loss to supervise the  $3D$  coordinates of hand vertices and MSE loss to supervise the  $2D$  projection of vertices:

$$L_v = \sum_{i=1}^N \|\mathbf{V}_{h,i} - \mathbf{V}_{h,i}^{GT}\|_1 + \|\Pi(V_{h,i}) - \Pi(V_{h,i}^{GT})\|_2^2, \quad (11)$$

where  $V_{h,i}$  is  $i$ -th vertex,  $h = L, R$  means left or right hand, and  $\Pi$  is the  $2D$  projection operation. Vertex loss is applied to each submesh.

**Regressed Joint Loss** By multiplying the predefined joint regression matrix  $J$ , hand joints can be regressed from the predicted hand vertices. The joint error is penalized by the following loss:

$$L_J = \sum_{i=1}^V \|JV_{h,i} - JV_{h,i}^{GT}\|_1 + \sum_{i=1}^V \|\Pi(JV_{h,i}) - \Pi(JV_{h,i}^{GT})\|_2^2. \quad (12)$$

**Mesh Smooth Loss** To ensure the geometric smoothness of the predicted vertices, two different smooth losses are applied. First, we regularize the normal consistency between the predicted and the ground truth mesh:

$$L_n = \sum_{f=1}^F \sum_{e=1}^3 \|e_{f,i,h} \cdot n_{f,h}^{GT}\|_1, \quad (13)$$

where  $f$  is the face index of the hand mesh,  $e_{f,i}(i = 1, 2, 3)$  are the three edges of face  $f$  and  $n_f^{GT}$  is the normal vector of this face calculated from the ground truth mesh. Second, we minimize the  $L1$  distance of each edge length between the predicted mesh and the ground truth mesh:

$$L_e = \sum_{e=1}^E \|e_{i,h} - e_{i,h}^{GT}\|_1. \quad (14)$$

## 5 Experiment

### 5.1 Experimental Settings

**Implementation Details** Our network is implemented using PyTorch. The network is trained in an end-to-end manner.

**Training Details** The proposed model is trained using the Adam optimizer [18] on 4 NVIDIA RTX 2080Ti GPUs with the minibatch size for each GPU set as 32. The whole training takes 100 epochs across 2.5 days, with the learning rate decaying to  $1 \times 10^{-5}$  at the 50-th epoch from the initial rate  $1 \times 10^{-4}$ . During training, data augmentations including scaling, rotation, random horizontal flip and color jittering are applied.

**Evaluation Metrics** To evaluate both the pose and shape accuracy of reconstructed hands, we compare the mean per joint position error (MPJPE) and mean per vertex position error (MPVPE) in millimeters. For fair comparison, we follow Two-Hands [49] to scale the length of the middle metacarpal of each hand to 9.5cm during training and rescale it back to the ground truth bone length during evaluation. This is performed after root joint alignment of each hand.

### 5.2 Datasets

**InterHand2.6M Dataset [27]** As the only dataset with two-hand mesh annotation, all networks in this paper are trained on InterHand2.6M [27]. As we only focus on two-hand reconstruction, we pick out the interacting two-hand (IH) data with both human and machine (H+M) annotated, and discard invalid labeling according to the hand type valid annotation provided by [27]. Ultimately, 366K training samples and 261K testing samples from InterHand2.6M are utilized. At preprocessing, we crop out the hand region according to the 2D projection of hand vertices and resize it to 256 × 256 resolution.

### 5.3 Quantitative Results

We first compare our proposed mobile network with the state-of-the-art two-hand reconstruction methods and recent two-hand reconstruction methods. The first model [27] regresses 3D skeletons of two hands directly. The second model [45] predicts the pose and shape parameters of two MANO [31] models. The third model [21] predicts the vertex of interacting-hands with graph and attention modules. For a fair comparison, we run their released source code on the same subset of Inter-Hand2.6M [27]. Comparison results are shown in Table 1. Figure 6 shows the results of our proposed model. It is clearly shown in Table 1 that our method achieved comparable MPJPE and MPVPE as the state-of-the-art models. Furthermore, we reduces the flops to  $0.47GFlops$  while the flops of the state-of-the-art models are around  $10GFlops$  or higher value.

**Table 1.** Comparison with the state-of-the-art models on performance and flops. The mean per joint position error (MPJPE) and mean per vertex position error (MPVPE) are calculated in millimeters. The flops are calculated in GFlops.

Model	MPJPE	MPVPE	Total flops	Image part	Pose part
Inter-Hand [27]	16.00	—	19.49	5.37	14.12
Two-Hand-Shape [45]	13.48	13.95	28.98	9.52	19.46
Intag-Hand [21]	8.79	9.03	8.42	7.36	1.06
Ours	12.56	12.37	0.47	0.25	0.22

## 6 Discussion

### 6.1 Conclusion

We present the proposed mobile method to reconstruct two interacting hands from a single RGB image. In this paper, we first introduce a lightweight feature attention module to extract both local occlusion representation and global image patch representation in a coarse-to-fine manner. We next propose a cross image and graph bridge module to fuse image context and hand vertex. Finally, we propose a lightweight cross attention mechanism which uses element-wise operation for cross attention of two hands. Comprehensive experiments demonstrate the comparable performance of our network on InterHand2.6M dataset, and verify the effectiveness and practicability of the proposed model in the real-time applications with low flops.

### 6.2 Limitation

The major limitation of our method is the high MPJPE and MPVPE. The proposed mobile modules reduce the flops while increase the error at the same time. We are studying efficient methods to further reduce the error for mobile application of two-hand reconstruction.



**Fig. 6.** Illustrations for interacting hand reconstruction by our proposed model.

## References

1. Baek, S., Kim, K.I., Kim, T.K.: Pushing the envelope for rgb-based dense 3d hand pose estimation via neural rendering. In: Proceedings of the IEEE/CVF Conference on Computer Vision and Pattern Recognition. pp. 1067–1076 (2019)
2. Boukhayma, A., Bem, R.d., Torr, P.H.: 3d hand shape and pose from images in the wild. In: Proceedings of the IEEE/CVF Conference on Computer Vision and Pattern Recognition. pp. 10843–10852 (2019)
3. Cai, Y., Ge, L., Cai, J., Yuan, J.: Weakly-supervised 3d hand pose estimation from monocular rgb images. In: Proceedings of the European Conference on Computer Vision (ECCV). pp. 666–682 (2018)
4. Chen, X., Liu, Y., Ma, C., Chang, J., Wang, H., Chen, T., Guo, X., Wan, P., Zheng, W.: Camera-space hand mesh recovery via semantic aggregation and adaptive 2d-1d registration. In: Proceedings of the IEEE/CVF Conference on Computer Vision and Pattern Recognition. pp. 13274–13283 (2021)
5. Chen, Y., Dai, X., Chen, D., Liu, M., Dong, X., Yuan, L., Liu, Z.: Mobile-former: Bridging mobilenet and transformer. In: Proceedings of the IEEE/CVF Conference on Computer Vision and Pattern Recognition. pp. 5270–5279 (2022)
6. Choutas, V., Pavlakos, G., Bolkart, T., Tzionas, D., Black, M.J.: Monocular expressive body regression through body-driven attention. In: European Conference on Computer Vision. pp. 20–40. Springer (2020)
7. Dong, X., Bao, J., Chen, D., Zhang, W., Yu, N., Yuan, L., Chen, D., Guo, B.: Cswin transformer: A general vision transformer backbone with cross-shaped windows. In: Proceedings of the IEEE/CVF Conference on Computer Vision and Pattern Recognition. pp. 12124–12134 (2022)
8. Fan, Z., Spurr, A., Kocabas, M., Tang, S., Black, M.J., Hilliges, O.: Learning to disambiguate strongly interacting hands via probabilistic per-pixel part segmentation. In: 2021 International Conference on 3D Vision (3DV). pp. 1–10. IEEE (2021)
9. Ge, L., Ren, Z., Li, Y., Xue, Z., Wang, Y., Cai, J., Yuan, J.: 3d hand shape and pose estimation from a single rgb image. In: Proceedings of the IEEE/CVF Conference on Computer Vision and Pattern Recognition. pp. 10833–10842 (2019)
10. Han, S., Liu, B., Cabezas, R., Twigg, C.D., Zhang, P., Petkau, J., Yu, T.H., Tai, C.J., Akbay, M., Wang, Z., et al.: Megatrack: monochrome egocentric articulated hand-tracking for virtual reality. ACM Transactions on Graphics (ToG) **39**(4), 87–1 (2020)
11. He, K., Zhang, X., Ren, S., Sun, J.: Deep residual learning for image recognition. In: Proceedings of the IEEE conference on computer vision and pattern recognition. pp. 770–778 (2016)
12. Heap, T., Hogg, D.: Towards 3d hand tracking using a deformable model. In: Proceedings of the Second International Conference on Automatic Face and Gesture Recognition. pp. 140–145. Ieee (1996)
13. Howard, A., Sandler, M., Chu, G., Chen, L.C., Chen, B., Tan, M., Wang, W., Zhu, Y., Pang, R., Vasudevan, V., et al.: Searching for mobilenetv3. In: Proceedings of the IEEE/CVF international conference on computer vision. pp. 1314–1324 (2019)
14. Howard, A.G., Zhu, M., Chen, B., Kalenichenko, D., Wang, W., Weyand, T., Andreetto, M., Adam, H.: Mobilenets: Efficient convolutional neural networks for mobile vision applications. arXiv preprint arXiv:1704.04861 (2017)
15. Joo, H., Liu, H., Tan, L., Gui, L., Nabbe, B., Matthews, I., Kanade, T., Nobuhara, S., Sheikh, Y.: Panoptic studio: A massively multiview system for social motion

capture. In: Proceedings of the IEEE International Conference on Computer Vision. pp. 3334–3342 (2015)

- 16. Joo, H., Simon, T., Sheikh, Y.: Total capture: A 3d deformation model for tracking faces, hands, and bodies. In: Proceedings of the IEEE conference on computer vision and pattern recognition. pp. 8320–8329 (2018)
- 17. Kim, D.U., Kim, K.I., Baek, S.: End-to-end detection and pose estimation of two interacting hands. In: Proceedings of the IEEE/CVF International Conference on Computer Vision. pp. 11189–11198 (2021)
- 18. Kingma, D.P., Ba, J.: Adam: A method for stochastic optimization. arXiv preprint arXiv:1412.6980 (2014)
- 19. Kulon, D., Guler, R.A., Kokkinos, I., Bronstein, M.M., Zafeiriou, S.: Weakly-supervised mesh-convolutional hand reconstruction in the wild. In: Proceedings of the IEEE/CVF conference on computer vision and pattern recognition. pp. 4990–5000 (2020)
- 20. Kyriazis, N., Argyros, A.: Scalable 3d tracking of multiple interacting objects. In: Proceedings of the IEEE Conference on Computer Vision and Pattern Recognition. pp. 3430–3437 (2014)
- 21. Li, M., An, L., Zhang, H., Wu, L., Chen, F., Yu, T., Liu, Y.: Interacting attention graph for single image two-hand reconstruction. In: Proceedings of the IEEE/CVF Conference on Computer Vision and Pattern Recognition. pp. 2761–2770 (2022)
- 22. Lin, K., Wang, L., Liu, Z.: End-to-end human pose and mesh reconstruction with transformers. In: Proceedings of the IEEE/CVF Conference on Computer Vision and Pattern Recognition. pp. 1954–1963 (2021)
- 23. Lin, K., Wang, L., Liu, Z.: Mesh graphomer. In: Proceedings of the IEEE/CVF International Conference on Computer Vision. pp. 12939–12948 (2021)
- 24. Liu, Z., Lin, Y., Cao, Y., Hu, H., Wei, Y., Zhang, Z., Lin, S., Guo, B.: Swin transformer: Hierarchical vision transformer using shifted windows. In: Proceedings of the IEEE/CVF International Conference on Computer Vision. pp. 10012–10022 (2021)
- 25. Mehta, S., Rastegari, M.: Mobilevit: light-weight, general-purpose, and mobile-friendly vision transformer. arXiv preprint arXiv:2110.02178 (2021)
- 26. Mehta, S., Rastegari, M.: Separable self-attention for mobile vision transformers. arXiv preprint arXiv:2206.02680 (2022)
- 27. Moon, G., Yu, S.I., Wen, H., Shiratori, T., Lee, K.M.: Interhand2. 6m: A dataset and baseline for 3d interacting hand pose estimation from a single rgb image. In: European Conference on Computer Vision. pp. 548–564. Springer (2020)
- 28. Mueller, F., Bernard, F., Sotnychenko, O., Mehta, D., Sridhar, S., Casas, D., Theobalt, C.: Ganerated hands for real-time 3d hand tracking from monocular rgb. In: Proceedings of the IEEE Conference on Computer Vision and Pattern Recognition. pp. 49–59 (2018)
- 29. Mueller, F., Davis, M., Bernard, F., Sotnychenko, O., Verschoor, M., Otaduy, M.A., Casas, D., Theobalt, C.: Real-time pose and shape reconstruction of two interacting hands with a single depth camera. ACM Transactions on Graphics (ToG) **38**(4), 1–13 (2019)
- 30. Oikonomidis, I., Kyriazis, N., Argyros, A.A.: Tracking the articulated motion of two strongly interacting hands. In: 2012 IEEE conference on computer vision and pattern recognition. pp. 1862–1869. IEEE (2012)
- 31. Romero, J., Tzionas, D., Black, M.J.: Embodied hands: Modeling and capturing hands and bodies together. arXiv preprint arXiv:2201.02610 (2022)

32. Rong, Y., Shiratori, T., Joo, H.: Frankmocap: Fast monocular 3d hand and body motion capture by regression and integration. arXiv preprint arXiv:2008.08324 (2020)
33. Rong, Y., Wang, J., Liu, Z., Loy, C.C.: Monocular 3d reconstruction of interacting hands via collision-aware factorized refinements. In: 2021 International Conference on 3D Vision (3DV). pp. 432–441. IEEE (2021)
34. Sandler, M., Howard, A., Zhu, M., Zhmoginov, A., Chen, L.C.: Mobilenetv2: Inverted residuals and linear bottlenecks. In: Proceedings of the IEEE conference on computer vision and pattern recognition. pp. 4510–4520 (2018)
35. Simon, T., Joo, H., Matthews, I., Sheikh, Y.: Hand keypoint detection in single images using multiview bootstrapping. In: Proceedings of the IEEE conference on Computer Vision and Pattern Recognition. pp. 1145–1153 (2017)
36. Spurr, A., Song, J., Park, S., Hilliges, O.: Cross-modal deep variational hand pose estimation. In: Proceedings of the IEEE conference on computer vision and pattern recognition. pp. 89–98 (2018)
37. Tang, X., Wang, T., Fu, C.W.: Towards accurate alignment in real-time 3d hand-mesh reconstruction. In: Proceedings of the IEEE/CVF International Conference on Computer Vision. pp. 11698–11707 (2021)
38. Taylor, J., Tankovich, V., Tang, D., Keskin, C., Kim, D., Davidson, P., Kowdle, A., Izadi, S.: Articulated distance fields for ultra-fast tracking of hands interacting. ACM Transactions on Graphics (TOG) **36**(6), 1–12 (2017)
39. Touvron, H., Cord, M., Douze, M., Massa, F., Sablayrolles, A., Jégou, H.: Training data-efficient image transformers & distillation through attention. In: International Conference on Machine Learning. pp. 10347–10357. PMLR (2021)
40. Tzionas, D., Ballan, L., Srikantha, A., Aponte, P., Pollefeys, M., Gall, J.: Capturing hands in action using discriminative salient points and physics simulation. International Journal of Computer Vision **118**(2), 172–193 (2016)
41. Wang, J., Mueller, F., Bernard, F., Sorli, S., Sotnychenko, O., Qian, N., Otaduy, M.A., Casas, D., Theobalt, C.: Rgb2hands: real-time tracking of 3d hand interactions from monocular rgb video. ACM Transactions on Graphics (ToG) **39**(6), 1–16 (2020)
42. Wang, Y., Min, J., Zhang, J., Liu, Y., Xu, F., Dai, Q., Chai, J.: Video-based hand manipulation capture through composite motion control. ACM Transactions on Graphics (TOG) **32**(4), 1–14 (2013)
43. Xiang, D., Joo, H., Sheikh, Y.: Monocular total capture: Posing face, body, and hands in the wild. In: Proceedings of the IEEE/CVF conference on computer vision and pattern recognition. pp. 10965–10974 (2019)
44. Xiao, B., Wu, H., Wei, Y.: Simple baselines for human pose estimation and tracking. In: Proceedings of the European conference on computer vision (ECCV). pp. 466–481 (2018)
45. Zhang, B., Wang, Y., Deng, X., Zhang, Y., Tan, P., Ma, C., Wang, H.: Interacting two-hand 3d pose and shape reconstruction from single color image. In: Proceedings of the IEEE/CVF International Conference on Computer Vision. pp. 11354–11363 (2021)
46. Zhang, F., Bazarevsky, V., Vakunov, A., Tkachenka, A., Sung, G., Chang, C.L., Grundmann, M.: Mediapipe hands: On-device real-time hand tracking. arXiv preprint arXiv:2006.10214 (2020)
47. Zhang, H., Tian, Y., Zhou, X., Ouyang, W., Liu, Y., Wang, L., Sun, Z.: Pymaf: 3d human pose and shape regression with pyramidal mesh alignment feedback loop. In: Proceedings of the IEEE/CVF International Conference on Computer Vision. pp. 11446–11456 (2021)

48. Zhang, X., Huang, H., Tan, J., Xu, H., Yang, C., Peng, G., Wang, L., Liu, J.: Hand image understanding via deep multi-task learning. In: Proceedings of the IEEE/CVF International Conference on Computer Vision. pp. 11281–11292 (2021)
49. Zhang, X., Li, Q., Mo, H., Zhang, W., Zheng, W.: End-to-end hand mesh recovery from a monocular rgb image. In: Proceedings of the IEEE/CVF International Conference on Computer Vision. pp. 2354–2364 (2019)
50. Zhang, Y., Li, Z., An, L., Li, M., Yu, T., Liu, Y.: Lightweight multi-person total motion capture using sparse multi-view cameras. In: Proceedings of the IEEE/CVF International Conference on Computer Vision. pp. 5560–5569 (2021)
51. Zhou, Y., Habermann, M., Habibie, I., Tewari, A., Theobalt, C., Xu, F.: Monocular real-time full body capture with inter-part correlations. In: Proceedings of the IEEE/CVF Conference on Computer Vision and Pattern Recognition. pp. 4811–4822 (2021)
52. Zhou, Y., Habermann, M., Xu, W., Habibie, I., Theobalt, C., Xu, F.: Monocular real-time hand shape and motion capture using multi-modal data. In: Proceedings of the IEEE/CVF Conference on Computer Vision and Pattern Recognition. pp. 5346–5355 (2020)
53. Zimmermann, C., Brox, T.: Learning to estimate 3d hand pose from single rgb images. In: Proceedings of the IEEE international conference on computer vision. pp. 4903–4911 (2017)
54. Zimmermann, C., Ceylan, D., Yang, J., Russell, B., Argus, M., Brox, T.: Freihand: A dataset for markerless capture of hand pose and shape from single rgb images. In: Proceedings of the IEEE/CVF International Conference on Computer Vision. pp. 813–822 (2019)